Website : jurnal.umj.ac.id/index.php/icecream

# Numerical Studies of Liquid Properties Effect on The Inception of Flooding in a Model of 1/30 Hot Leg PWR

**Rafid Zulfiadib[1] , Deendarlianto[1*]**

[1] *Department of Mechanical and Industrial Engineering, Gadjah Mada University, Indonesia*
[*] *Email address of corresponding author: deendarlianto@ugm.ac.id*

**ABSTRACT**

An operation of nuclear power plant such as Pressurized Water Reactor (PWR) requires a high standard of safety management. In order to prevent the accidental scenario such as Loss of Coolant Accident (LOCA), the characteristic of flooding regime during CCFL should be investigated. This present study covers a numerical simulation on the effect of liquid properties during the inception of flooding or CCFL in a model of 1/30 hot leg PWR. Transient numerical simulations are performed using ANSYS Fluent 2020 R2 software with the Volume of Fluid (VOF) method to model a counter-current two-phase flow in the hot leg pipe. The geometry used is the German Konvoi type with a scale of 1/30. The diameter and the length of the hot leg are D = 25.4 mm and L = 455 mm respectively, resulting in a ratio of L/D = 17.91. The gas fluid used is air while the liquid fluid used is distilled water with the addition of %wt glycerin 40% and 60%. The results showed that the increase in liquid viscosity caused flooding initiation to occur at lower gas superficial velocities. While a decrease in surface tension causing the flooding to occur at lower gas flow rates.



Keywords: Counter Current Flow Limitation, Onset of Flooding, Pressurized Water Reactor, VOF, CICSAM

## 1. Introduction

PWR is a type of nuclear reactor that keeps the working fluid under saturated conditions. In PWR operation, the working fluid temperature is maintained in the liquid phase up to 325℃ at a pressure of 15 Mpa [4]. Under these conditions, the saturation point of pressure and temperature is 22.06 Mpa and 374.1 ℃. If a leak occurs in the primary circuit, the reactor will experience a drastic pressure drop, causing a vaporization phenomenon of coolant in the RPV. This phenomenon is called LOCA (loss of coolant accident). If the coolant level is below the hot leg, the vapor formed due to the pressure drop will flow to the steam generator through the hot leg pipe. As a result, there will be a counter-current two-phase flow in the hot leg pipe. If the gas flow rate is too high, the liquid will begin to stop and the direction will reverse following the direction of the gas [1]. This phenomenon is referred to as counter-current flow limitation (CCFL) or flooding. The onset of flooding is defined as the CCFL stability limit which is indicated by the maximum air mass flow rate at which the downward flowing liquid mass flow rate equals the liquid mass flow rate at the inlet [3].

The CCFL phenomenon has an important role in the safety sector of nuclear reactor operations. For this reason, further research is needed that corresponds to several parameters that could affect the CCFL phenomenon. From a number of studies that have been conducted, many studies discuss the physical properties of fluids in the form of differences in fluid viscosity, as well as surface tension on flooding initiation. From these studies, it is found that an increase in liquid viscosity causes a decrease in the superficial velocity of gas flooding [5]. On the other hand, Astyanto et al. [2] revealed that the effect of differences in surface tension did not significantly affect the characteristics of CCFL when compared to the effect of differences in liquid viscosity.

Research on the effect of fluid viscosity on the onset of flooding was conducted by Suzuki & Ueda, [8]. The research was conducted experimentally using vertical pipes and the fluids used were water, glycerol solution, and sec.-octyl alcohol solution. The results showed that the flooding velocity increased as the pipe length decreased and as the viscosity increased. On the other hand, research on the effect of fluid viscosity was also conducted by Zapke &

Kroger [9]. From the results of this study, different results were found to the research conducted by Suzuki & Ueda, [8]. The results of Zapke & Kroger [9] found that the thickness of the liquid film increases as the viscosity of the liquid increases. The increase in liquid film thickness can cause an increase in gas velocity because the channel cross-sectional area decreases, thus increasing the drag force. This can cause the flooding initiation phenomenon to occur at smaller gas superficial velocities.

Ousaka et al., [6] conducted a study using water and oleic acid sodium solution as the liquid phase and air as the gas phase. The results showed that surface tension can affect the characteristics of the beginning of flooding. An increase in surface tension value can lead to an increase in gas flooding speed. This is because the liquid hold-up increases along with the decrease in the surface to produce a greater drag force, so that the flooding phenomenon will occur at low gas flow rates and at low surface tension. On the other hand, Pantzali et al. [7] in their research, found that surface tension has less influence than other physical properties. This is evidenced by observations on channel geometries with inclination angles of 30°, 45°, and 60°. From the research results, it is stated that surface tension has a stabilizing effect on the liquid and gas interface. Low surface tension causes large fluctuations on the surface resulting in higher waves. Flooding starts when the drag force on the standing wave in the pipe outlet area becomes larger to resist gravity, bringing the wave crawling up.

Based on several studies that have been conducted regarding the physical properties of fluids to the flooding phenomenon in the PWR hot leg, it is found that there are still some gaps between the research results. This is due to differences in interpretation of experimental results, where differences in experimental methods and channel geometry shapes, both rectangular and circular, also have a significant influence. In addition, some studies have only been carried out at certain scales, with the most research being on the geometry of hot leg PWR with a scale of 1/15 and 1/3, while at a scale of 1/30 there has not been many numerical researchs. This research will focus on the characteristics of the onset of flooding against the differences in the physical properties of the liquid used in the form of changes in viscosity and surface tension. The results of this numerical simulation research are then used to enrich the experimental data that has been carried out by Astyanto et al., [2].

## 2. Material and Methods

### *2.1. Numerical Modelling*

In this study, transient numerical simulations are performed on a 3-Dimensional geometry using a pressure-based solver. The interfacial distributions are tracked using Volume of Fluid (VOF) method. The Pressure-Velocity Coupling is made using PISO scheme with neighbor correction. Spatial discretization of volume fraction and pressure are made using the CICSAM scheme and PRESTO scheme respectively. 2nd order upwind scheme is used for spatial discretization of momentum, whereas 1st order upwind scheme is used for spatial discretization of turbulent kinetic energy (k) and specific dissipation rate (ω). In this study, liquid is considered as the primary phase, whereas gas is the secondary phase.

#### *2.1.1. Governing Equations*

Using a fractional scheme to track the free boundary where the fluid moves through a fixed computational mesh, the VOF method divides the computational domain into small cells. In this method, it is assumed that the fluids involved in the flow being modeled are immiscible, but can reside within the computational domain, intersecting each other on a scale determined by the volumetric size of the computational mesh. Each cell is assigned a value between zero and one indicating the volume fraction of fluid present in it. This value will be one if the cell is filled with the gas phase, zero if it is filled with the liquid phase, and between zero and one if the cell is filled with the interface. As a result, this technique can handle changes in interface topology.

In the VOF method, the density and viscosity of each cell are calculated using an average that is affected by the volume fraction distribution with the following equation:

$$\rho = \alpha\rho_l + (1-\alpha)\rho_g \quad 2.1$$

$$\mu = \alpha\mu_l + (1-\alpha)\mu_g \quad 2.2$$

For incompressible and adiabatic two-phase flow, the density and viscosity of the fluid are constant. Thus, the continuity and momentum equations are written in the following equations:

$$\nabla \cdot \mathrm{U} = 0 \quad 2.3$$

$$\frac{\partial \alpha}{\partial t} + \nabla \cdot (\alpha U) = 0 \quad 2.4$$

$$\frac{\partial(\rho U)}{\partial t} + \nabla \cdot (\rho U^2) = -\nabla P + \mu \nabla^2 U + \rho g + \sigma k \nabla \alpha \quad 2.5$$

where, k is the average curvature of the fluid interface, and $\alpha$ is the void fraction.

### *2.1.2. Meshing*

The mesh creation process in this research is made with a hexahedral mesh type with complex shapes. For this reason, supporting ICEM CFD is needed to create a mesh with a hexahedral pattern with complex geometry, where the domain discretization process is done manually by creating a grid based on the hexa-blocking method. The number of elements generated is 120,588 elements.

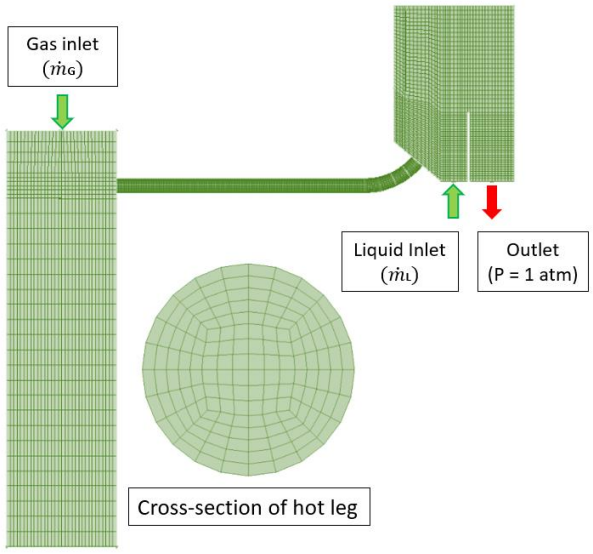


Figure 1: Hexahedral mesh using ICEM CFD

### *2.1.3. Boundary Condition*

In this study, compressed air from the gas inlet channel is used to replace water vapor as the gas phase, while distilled water with a mixture of glycerin is used to replace condensate as the liquid phase. To simulate the phenomenon of liquid-to-gas phase change due to the drastic pressure drop in the RPV under actual conditions in the PWR primary circuit, this adiabatic study uses a gradually increasing gas discharge as a representation of the increasing liquid-to-gas change. In the numerical simulation process, the gas discharge was increased gradually at intervals of 0,35 m/s every 25 seconds, while the liquid discharge was kept fixed throughout the process. The gas phase used is air, while the liquid phase used is distilled water (DW) with the addition of %wt glycerin 40% (G40) and 60% (G60). The properties of each type of fluid are shown in Table 1.

Table 1: Fluid Properties at ambient temperature

| Type of Fluid | Density (kg/m$^3$) | Dynamic Viscosity (kg/m.s) | Surface Tension (N/m) |
|---|---|---|---|
| Air | 1.15 | $1.87 \times 10^{-5}$ | - |
| DW | 977.34 | $7.97 \times 10^{-4}$ | 0.072 |
| G40 | 1058.13 | $31.67 \times 10^{-4}$ | 0.064 |
| G60 | 1126.34 | $95.72 \times 10^{-4}$ | 0.058 |

## 3. Results and Discussions

### *3.1 Data Validation*

The data validation in this study is based on the flooding onset graph displayed in the relationship between the superficial velocity of gas ($J_G$) and the superficial velocity of liquid ($J_L$). Figure 2 shows the onset of flooding data between DW-air, G40-air, and G60-air which is then compared with the experimental data in Astyanto's research (2022). From the results of the graph, it can be seen that the increase in numerical simulation results in the DW fluid type has a similar trend to the experimental results from Astyanto et al. [2]. However, there are some differences in the data towards the starting condition point of flooding. This is because the difference in flooding initiation time is only a difference of approximately 5 seconds before the superficial gas increase at 25 second intervals occurs. Thus, at superficial velocities JL = 0.015 m/s and JL = 0.06 m/s the flooding initiation in the numerical simulation is achieved faster. However, the numerical data is still considered valid because it has a similar data trend and has an unconsiderable difference in data results, which is only one interval difference.

### *3.2 The Inception of Flooding Characteristics*

The flooding initiation characteristics can be displayed in the relationship between non dimensional gas superficial velocity $(J_G^*)^{0.5}$

and non dimensional liquid superficial velocity $(J_L^*)^{0.5}$. From the graph in Figure 3, it can be seen that the viscosity of the liquid causes flooding initiation to occur at lower gas superficial velocities. An increase in liquid superficial velocity also causes flooding initiation to occur at lower gas superficial velocities. This shows similar results obtained in Zapke and Kroger [9] and Kinoshita et al. [5].

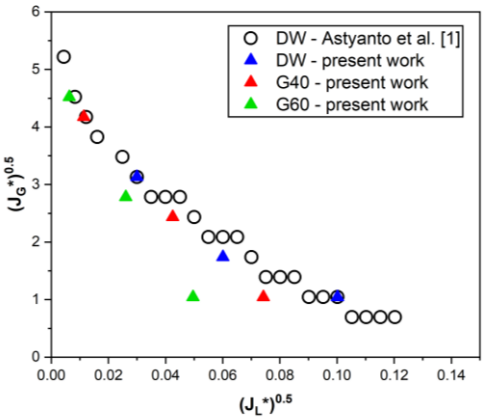


Figure 2: CCFL Characteristics

The inception of flooding can be indicated by a sudden pressure drop or pressure fluctuation. These fluctuations are caused by liquids that begin to reverse in direction following the direction of gas flow with a large waveform (LW) until a slug formation. The formed slug will cover the hotleg cross-sectional area and can cause the gas flow rate to the SGs to be obstructed.

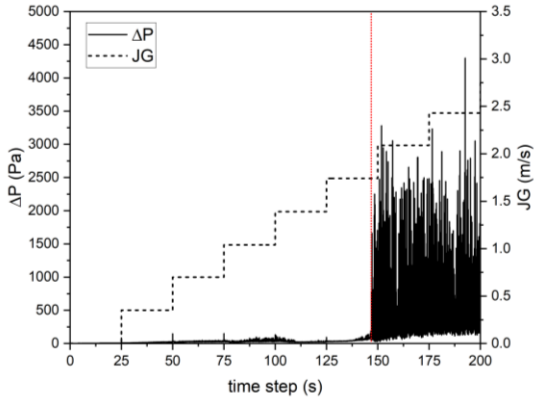


Figure 3: Pressure difference between RPVs and SGs during the inception of flooding at JL = 0.06 m/s

In Figure 3, it can be seen that flooding initiation occurs at $J_G$ = 1.74 m/s for the Air-DW variation. The pressure difference pattern after flooding will experience very significant fluctuations. This is because the slug flow that occurs in the hotleg channel initiates a roll wave. The roll wave flow pattern is then split into churn flow with chaotic patterns in the turn or riser area. When liquid blockage occurs, the pressure difference will increase drastically. Conversely, when the roll wave begins to descend there is a flow gap that opens again so that the pressure difference will decrease. This pattern occurs repeatedly resulting in forceful pressure fluctuations.

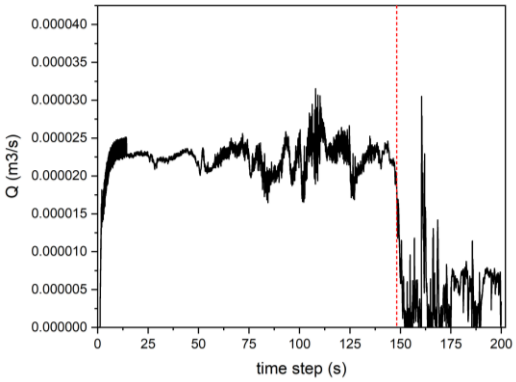


Figure 4: Volumetric flow rate of liquid through RPVs during the inception of flooding at $J_L$ = 0.06 m/s

Furthermore, at the onset of flooding, the volumetric flow rate of the liquid entering the RPVs will decrease drastically as shown in Figure 4. This also supports the hypothesis on the increase in pressure difference between RPVs and SGs due to the blocking area caused by slug flow in the hotleg channel. Then, shortly after a decrease in volumetric flow rate, there is a drastic surge in liquid discharge towards RPVs due to the momentum generated from the liquid wave towards the riser at a time step of 162 seconds. Thus, it makes the liquid discharge charge will reverse in direction towards RPVs with a larger amount.

### *3.3 Flow Patterns*

In the flow pattern shown in Figure 5, when only liquid is flowed, HJ is observed at the location of the hot leg end towards the RPVs. At $J_G$ = 1.04 m/s, the HJ is observed to shift towards the liquid inlet. Stratified flow with relatively similar characteristics along the horizontal section is still observed when the gas flows in the opposite direction to the liquid with a slight increase in flow rate. Then, at $J_G$ = 1.39 m/s large waves begin to form. At this condition, the interface along the HJ looks increasingly wavy in the direction of liquid flow. Slug formation begins to form at $J_G$ = 1.74 m/s which is the initiation of flooding with a significant increase in pressure difference. Then the formed slug initiates the formation of

roll wave until it reaches the churn flow at the riser. This churn flow pattern also proves the phenomenon of drastic pressure fluctuations at the time after flooding and will tend to decrease until it reaches zero liquid penetration.

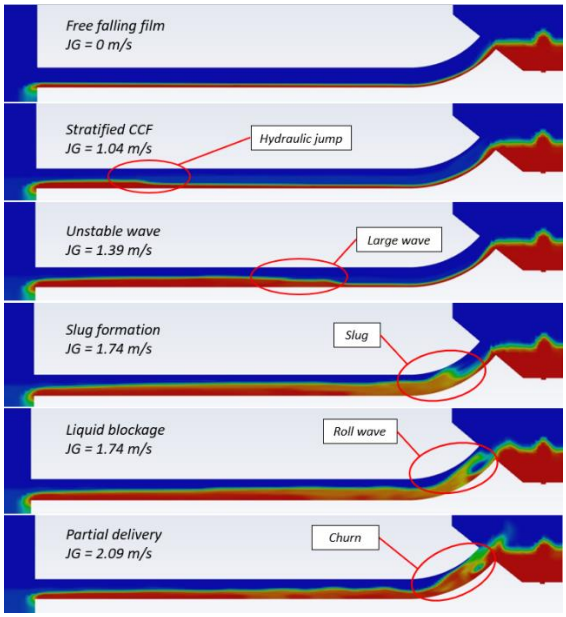


Figure 5: Volume fraction visualization during the inception of flooding at $J_L$ = 0.06 m/s

Figure 6 shows the locus of slugging graph for DW, G40, and G60 fluid variations. The parameter x/L represents the position along the hot leg channel, where x/L = 0 is the position of the horizontal pipe closest to the riser, while x/L = 1 is the position of the horizontal pipe furthest from the riser. The data shows that as the viscosity of the liquid increases, the locus of slugging shifts closer to the riser. This is because liquids with high viscosity will experience flow slowdown due to the large friction force on the hot leg wall. On the other hand, surface tension contributes to slug formation. In liquids that have low surface tension, the liquid hold-up will be greater. This then leads to an increased gas flow rate due to the narrowing of the pipe cross-sectional area. Thus, liquids with high viscosity and low surface tension will create slug formation earlier and will make flooding initiation occur at lower gas flow rates.

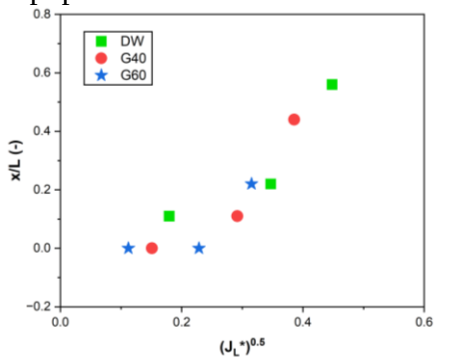


Figure 6: Locus of slugging

## 4. Conclusion

The influence of the liquid properties effect on the flooding initiation characteristics has been investigated using numerical simulation. The increase in liquid viscosity causes flooding initiation to occur at lower gas superficial velocities, where the increase in viscosity causes an increase in friction force on the hot leg wall which can cause the pressure difference between liquid and gas to increase. The increase in friction force on the hot leg wall also leads the hydraulic jump to shift closer to the riser. Surface tension affects liquid hold-up, where the lower the surface tension, the liquid hold-up will increase. The increase in liquid hold-up corresponds to the available area for the gas flow to pass through, where at high liquid hold-up the gas flow will accelerate and cause the start of flooding to be achieved at a lower gas flow rate.

## Acknowledgement

-

## References

[1] Al Issa, S., & MacIan, R. (2011). A review of CCFL phenomenon. *Annals of Nuclear Energy*, *38*(9), 1975-1819. https://doi.org/10.1016/j.anucene.2011.04.021

[2] Astyanto, A. H., Indarto, Kirkland, K. V., & Deendarlianto. (2022). An experimental study on the effect of liquid properties on the counter-current flow limitation (CCFL) during gas/liquid counter-current two-phase flow in a 1/30 scaled-down of Pressurized Water Reactor (PWR) hot leg geometry. *Nuclear Engineering and Design*, *399*(2), 112052. https://doi.org/10.1016/j.nucengdes.2022.112052

[3] Deendarlianto, Höhne, T., Lucas, D., Vallée, C., dan Zabala G., 2011, CFD studies on the phenomena around counter-current flow limitations of gas/liquid two-phase flow in a model of a PWR hot leg, *Nuclear Engineering Design*, *241*(12), hal. 5138–5148. https://doi.org/10.1016/j.nucengdes.2011.08.071

[4] Deendarlianto, Höhne, T., Lucas, D., & Vierow, K., 2012, Gas-liquid countercurrent two-phase flow in a PWR hot leg: A comprehensive research review, *Nuclear Engineering and Design, 243*(2), 214–233. https://doi.org/10.1016/j.nucengdes.2011.11.015

[5] Kinoshita, I., Nriai, T., Tomiyama, A., Lucas, D., & Murase, M., 2011, Effects of Liquid Properties on CCFL in a Scaled-Down Model of a PWR Hot Leg, *Journal of Power and Energy Systems, 5*(3), 316–329. https://doi.org/10.1299/jpes.5.316

[6] Ousaka, A/, Kariyasaki, A., & Fukano, T. (2006). Prediction of flooding gas velocity in gas-liquid counter-current two-phase flow in inclined pipes. *Nuclear Engineering and Design, 236*(12), page 1282-1292. https://doi.org/10.1016/j.nucengdes.2005.12.001

[7] Pantzali, M. N., Mouza, A. A., & Paras, S. V. (2007). Study of hydrodynamic characteristics of the liquid layer during counter- current flow in inclined small diameter tubes: the effect of liquid properties. *6th International Conference on Multiphase Flow, Leipzig, Germany., July*.

[8] Suzuki, S., & Ueda, T., 1977, Behaviour of liquid films and flooding in counter-current twophase flow-Part 1, Flow in circular tubes, *International Journal of Multiphase Flow, 3*(6), 517– 532.

[9] Zapke, A. dan Kröger, D. G., 1996, The influence of fluid properties and inlet geometry on flooding in vertical and inclined tubes, *International Journal of Multiphase Flow, 22*(3), page. 461–472.